PLOS GENETICS

RESEARCH ARTICLE

Tup1 is critical for transcriptional repression in Quiescence in *S. cerevisiae*

Thomas B. Bailey, Phaedra A. Whitty, Eric U. Selker [ID], Jeffrey. N. McKnight, Laura E. McKnight [ID] *

Institute of Molecular Biology, University of Oregon, Eugene, Oregon, United States of America

* lmcknigh@uoregon.edu

Abstract

Upon glucose starvation, *S. cerevisiae* shows a dramatic alteration in transcription, resulting in wide-scale repression of most genes and activation of some others. This coincides with an arrest of cellular proliferation. A subset of such cells enters quiescence, a reversible non-dividing state. Here, we demonstrate that the conserved transcriptional corepressor Tup1 is critical for transcriptional repression after glucose depletion. We show that Tup1-Ssn6 binds new targets upon glucose depletion, where it remains as the cells enter the G0 phase of the cell cycle. In addition, we show that Tup1 represses a variety of glucose metabolism and transport genes. We explored how Tup1 mediated repression is accomplished and demonstrated that Tup1 coordinates with the Rpd3L complex to deacetylate H3K23. We found that Tup1 coordinates with Isw2 to affect nucleosome positions at glucose transporter HXT family genes during G0. Finally, microscopy revealed that a quarter of cells with a Tup1 deletion contain multiple DAPI puncta. Taken together, these findings demonstrate the role of Tup1 in transcriptional reprogramming in response to environmental cues leading to the quiescent state.

Author summary

Quiescence is a very common and important state for the cells of many organisms, where cell functions 'pause' but can resume when the right conditions are met. Most microbes exist in a quiescent state and will start growing and dividing again in the presence of nutrients or other cues. In mammals, a quiescent state is used to maintain stem cell populations and cancer cells often evade treatment by entering quiescence. The budding yeast *Saccharomyces cerevisiae* is an excellent model for studying quiescence because we can easily isolate populations of quiescent cells. Since budding yeast share many proteins and cellular pathways with higher organisms, our findings are applicable to more complex systems, which may be relevant to maintenance of healthy cells or provide insight to treating disease states. We know that a hallmark of quiescence is reduced transcription, and we are interested in how this change occurs. We have examined how the protein Tup1 causes changes in gene expression in cellular quiescence. We also looked at how Tup1-dependent changes depend on other chromatin interacting factors, such as the histone deacetylase Rpd3, the transcription factor Xbp1, or the chromatin remodeling protein Isw2.

Introduction

Cellular quiescence is a non-proliferative cell state that appears conserved across all life [1–3]. Quiescent cells are distinct from other non-dividing cells, such as senescent and terminally differentiated cells, in that quiescent cells can return to a proliferative state if the right conditions are met. Quiescence is necessary for the survival of unicellular organisms in environments that are unfavorable for proliferation; in fact, most microbes in nature are quiescent [4,5]. In multicellular eukaryotes, quiescence plays a critical role in various cell types including stem cells, fibroblasts, and lymphocytes [3,6,7]. The inability to properly regulate quiescence can lead to cancer; additionally, cancer stem cells can become quiescent, leading to drug resistance and the ability to initiate relapse at a later time [8]. All quiescent cells have conserved characteristics including transcriptional repression, increased cell density, translational repression, and decreased cell metabolism [9–12]. Many of the components that regulate quiescence are found throughout life and likely have conserved functions; however, some of the fundamental ways cells regulate entry, exit, and maintenance of quiescence are not fully understood [13].

Saccharomyces cerevisiae is a well-established model organism for studying cellular quiescence because it can reliably produce a population of quiescent cells [10,12]. Quiescence is notoriously difficult to study in multicellular organisms due to the lack of quiescence-specific biomarkers and because it is difficult to determine which cells are quiescent until they begin dividing again. *S. cerevisiae* can produce a large population of quiescent cells that can be isolated by density centrifugation [14]. Additionally, budding yeast is capable of surviving mutations that would be lethal in higher order organisms, allowing study of critically important factors in the process of establishing quiescence [11,12]. Because many of the fundamental components that regulate the cell cycle are conserved between budding yeast and higher eukaryotes, we suspect that many players involved in cell cycle arrest are highly conserved.

Tup1-Ssn6 is a transcriptional corepressor complex that globally regulates many cell processes in *S. cerevisiae* [15]. Tup1 serves mostly as a repressor, although it can also induce gene expression in some contexts depending on its phosphorylation state [16,17]. Tup1 forms a complex with Ssn6 in which 3–4 Tup1 molecules associate with each Ssn6 molecule [18]. The structure of Tup1 contains an N-terminal helix, which facilitates oligomerization and interacts with histone tails, and a beta-propeller domain composed of seven WD40 domains, which interact with other proteins such as histone deacetylases and DNA binding factors [19]. While the detailed mechanism of repression by Tup1 is unknown, some relevant information is available. Tup1 is recruited by sequence-specific transcription factors to DNA [20], where it recruits histone deacetylases (HDACs) to generate hypoacetylated regions of chromatin, typically associated with transcriptional repression [21–24]. In addition to HDAC recruitment, Tup1 interacts directly with nucleosomes by binding histone H3 and H4 tails, preferentially to hypoacetylated tails, to stabilize +1 nucleosomes that have been repositioned by Isw2 [25–28]. Tup1 also interacts directly with the Mediator complex through its subunit Hrs1, potentially inhibiting it from transcribing into gene bodies [29]. Lastly, Tup1 is thought to influence transcription by blocking the recruitment of activating factors to chromatin [30,31].

Homologues of Tup1-Ssn6 found in higher eukaryotes include groucho in drosophila, grg in mice, and TLE1 in humans [32]. While the beta-propeller domain is well conserved in both sequence and structure, the sequence of the N-terminus is poorly conserved; however, it appears to be structurally conserved in simulations [33,34]. Cross-species interactions have been established, where TLE family proteins can pull down yeast Ssn6 from cellular lysate, suggesting strong conservation of structure and function [35,36]. Mice and flies exhibit severe developmental phenotypes in Groucho/TLE null or hypomorphic mutations [37].

Additionally, in humans TLE1 is currently being studied as both a cancer biomarker and a potential cancer therapeutic drug target [38,39]

During quiescence in yeast, it has been observed that nucleosomes are repositioned and histone tails are deacetylated [40,41]. Tup1 plays a role in histone deacetylation and chromatin remodeling in other contexts [21,28]; however, it is unclear whether Tup1 contributes to these processes in quiescence. Tup1 has been identified as a gene that is essential for viability of cells in G0 and is implicated in glucose repression in yeast, but there is no molecular mechanism to explain its role in these processes [42–46]. Here, we demonstrate that Tup1 is essential for repressing target genes in stationary phase by interacting with Rpd3 and Isw2 to generate regions of repressed chromatin. We also show that cells lacking Tup1 display morphological defects in stationary phase, suggestive of a possible role for Tup1 in mitosis.

Results

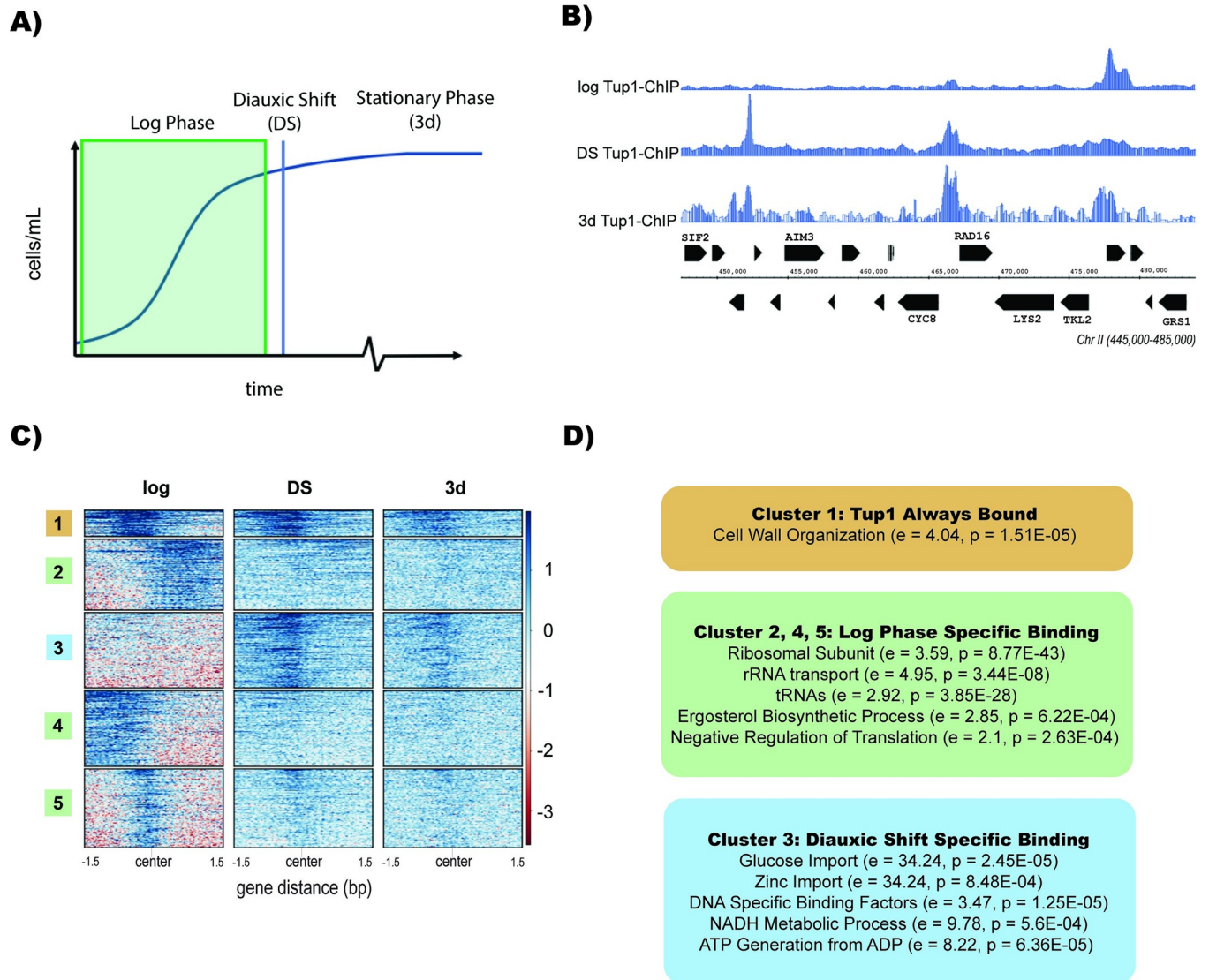### Tup1 Relocalizes After Glucose Starvation

Because Tup1 is a master regulator of many processes in *S. cerevisiae*, we sought to investigate the consequences of glucose starvation on Tup1 localization across the genome. We performed ChIP-Seq analysis on a Myc-tagged Tup1 strain during log phase, diauxic shift, and stationary phase (**Fig 1A**). Ideally, we would work with purified quiescent cells, but due to the unusual clumping of Tup1 deletion strains (**S1 Fig**), which is not alleviated by the addition of EDTA, it is impossible to isolate pure populations of quiescent cells. We therefore performed ChIP for Tup1 in stationary phase so that direct comparisons could be made to Δtup1 strains. However, we do anticipate that the findings in stationary phase translate to quiescence because we observed that a fraction of stationary cells in Tup1 knockout strains are viable and can re-enter the cell cycle when plated on glucose rich media. Additionally, we know that Tup1 knockouts have reduced viability in G0, indicating that Tup1 plays a critical role in quiescence.

In log phase, we observed Tup1 binding to the promoters of roughly 923 genes, including genes for ribosomal protein subunits, tRNAs, and cell wall organization (**Fig 1B and 1C**). During diauxic shift, we observed Tup1 at 174 new targets across the genome, where it persisted into stationary phase. Gene ontology analysis revealed that during diauxic shift, Tup1 binds to the promoters of sugar transmembrane transporters, carbohydrate kinases, ATP from ADP factors, zinc transporters, and DNA binding transcription factors (**Fig 1D**). Motif analysis revealed significant enrichment for binding motifs of 78 transcription factors, including Mig1, which is known to recruit Tup1 to sites of repression (**S1 Table**) [43, 47, 48].

Tup1 both activates and represses key targets for Quiescence initiation

Next, we sought to understand how Tup1 binding correlates with transcriptional changes upon glucose repression. We performed differential expression analysis on RNA-Seq datasets, comparing transcription between wild type and Tup1 knockout strains during diauxic shift and stationary phase (**Fig 2A**). We were able to detect differential expression of 2102 genes in diauxic shift and 2999 genes during stationary phase in the Tup1 deletion, suggestive of Tup1's role in altering transcriptional programming during glucose exhaustion. Of the genes that were significantly differentially expressed in diauxic shift, nearly 60% had a 2-fold increase in expression, while the remaining 40% showed significant reduction in expression (**Fig 2A**). During stationary phase, only slightly more genes showed increased expression than showed decreased expression (approximately 52% versus 48%). Among genes that are repressed by Tup1, 787 were repressed in both diauxic shift and stationary phase (**Fig 2B**).

A previous screen for genes required for quiescence in yeast found 137 deletion mutants that were unable to form a quiescent cell population [49]. In our experiments, Tup1 was found

Fig 1. Tup1 Relocalizes After Glucose Starvation. (A) Illustration of a yeast growth curve indicating diauxic shift (DS) and stationary phase (3d). (B) Integrated Genome Browser (IGB) tracks representative of Tup1-myc ChIP-Seq during log phase, diauxic shift, and stationary phase. Data are normalized to RPKM. (C) ChIP-Seq heatmap of Tup1 binding during log phase, diauxic shift, and stationary phase. Heatmap was clustered using deeptools and sorted by binding intensity. (D) Gene ontology analysis from GOrilla of Tup1 binding locations with relative enrichment (e) and p-value (p) indicated for each term.

https://doi.org/10.1371/journal.pgen.1010559.g001

to regulate expression of 57% of these genes, indicating that Tup1 plays a key role in transcriptional reprogramming during quiescence. Gene ontology analysis revealed that during diauxic shift, Tup1 represses genes associated with transmembrane transport and metabolism of carbohydrates (**Fig 2C**). We also observed Tup1 repressing genes implicated in transportation of amino acids, metal ions (Zn^{2+}, Mg^{2+}, Cu^{2+}, and Fe^{2+}), vitamins, and fatty acids. While transportation of fatty acids appears repressed, metabolism of fatty acids appears to be activated by Tup1. In addition to repressing transportation of many components, Tup1 apparently stalls translation by repressing expression of ribosomal protein subunits, ribosome biogenesis genes, and tRNA ligases. During stationary phase, Tup1 represses many of the same genes found in diauxic shift, and also represses additional gene sets including rRNAs and DNA transcription factors associated with gene activation.

A)
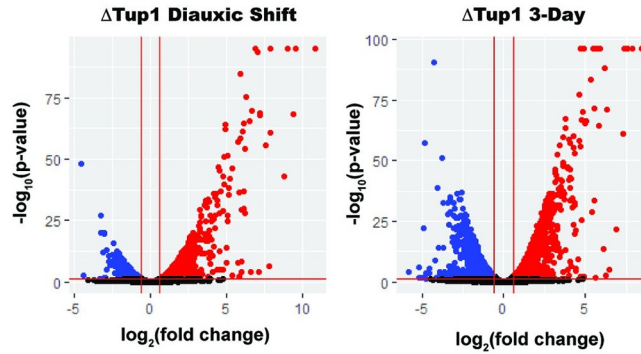
B)
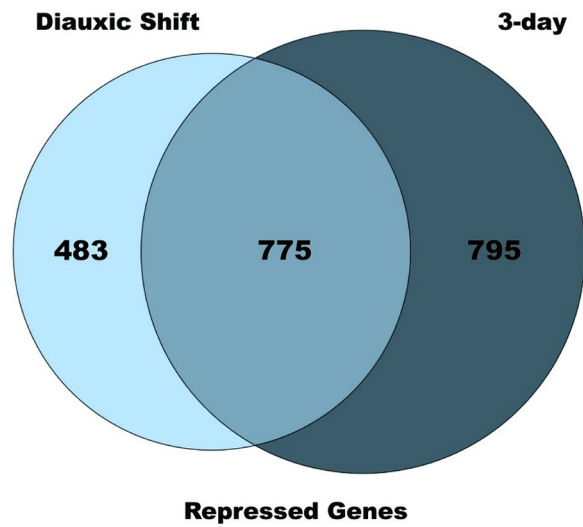
C)

Repressed by Tup1
Carbohydrate Transport (e = 2.29, p = 6.99E-06)
Ion Transport (e = 1.43, p = 7.58E-07)
rRNA and Ribosome Processing (e = 1.69, p = 5.64E-08)
Translation (e = 2.16, p = 6.51E-21)

Activated by Tup1
Fatty Acid Metabolism (e = 2.73, p = 2.63E-06)
Glyoxylate Cycle(e = 5.42, p = 2.63E-04)
Synaptonemal Complex (e = 3.19, p = 2.68E-05)
Golgi Transport (e = 1.60, p = 9.08E-06)

Fig 2. Tup1 Activates and Represses Key Targets for Quiescence Initiation. (A) Volcano plots of RNA-Seq differential expression data comparing a Tup1 deletion to wild type. Expression changes are based on two biological replicates. (B) Venn diagram comparing genes that are repressed by Tup1 in diauxic shift to those repressed in stationary phase. (C) Gene ontology analysis from GOrilla of transcripts affected by Tup1 in both diauxic shift and stationary phase with relative enrichment (e) and p-value (p) indicated for each term.

By comparing the results from RNA-Seq and ChIP-Seq, we found that Tup1 occupancy does not correlate solely with repression or activation of genes. For example, out of the 981 genes Tup1 releases from in DS, 35% have higher levels of expression in the Tup1 deletion and 25% have lower levels, while 40% are not significantly affected. Perhaps Tup1 release frees up binding for additional factors, which may be repressive or may induce transcription. Of the 176 genes where we detect Tup1 binding during DS, we find that 131 are differentially expressed. Most (60%) are repressed by Tup1 and less than 15% are activated, demonstrating that Tup1 recruitment to a site during diauxic shift is usually indicative of repression. Because the number of sites bound by Tup1 in the ChIP dataset does not match the number of repressed genes, it is likely that we are not detecting all Tup1 binding that occurs during diauxic shift; however, we do not believe that the inability to detect all instances of Tup1 binding fully accounts for this difference. We observed that Tup1 binds to and represses many DNA binding transcription factors including Hap1, Nrg1, and Mig1 (**S1 Table**) and downstream effects of the repression of these transcription factors may account for why there are more repressed targets in the RNA-Seq dataset compared to the ChIP-Seq dataset.
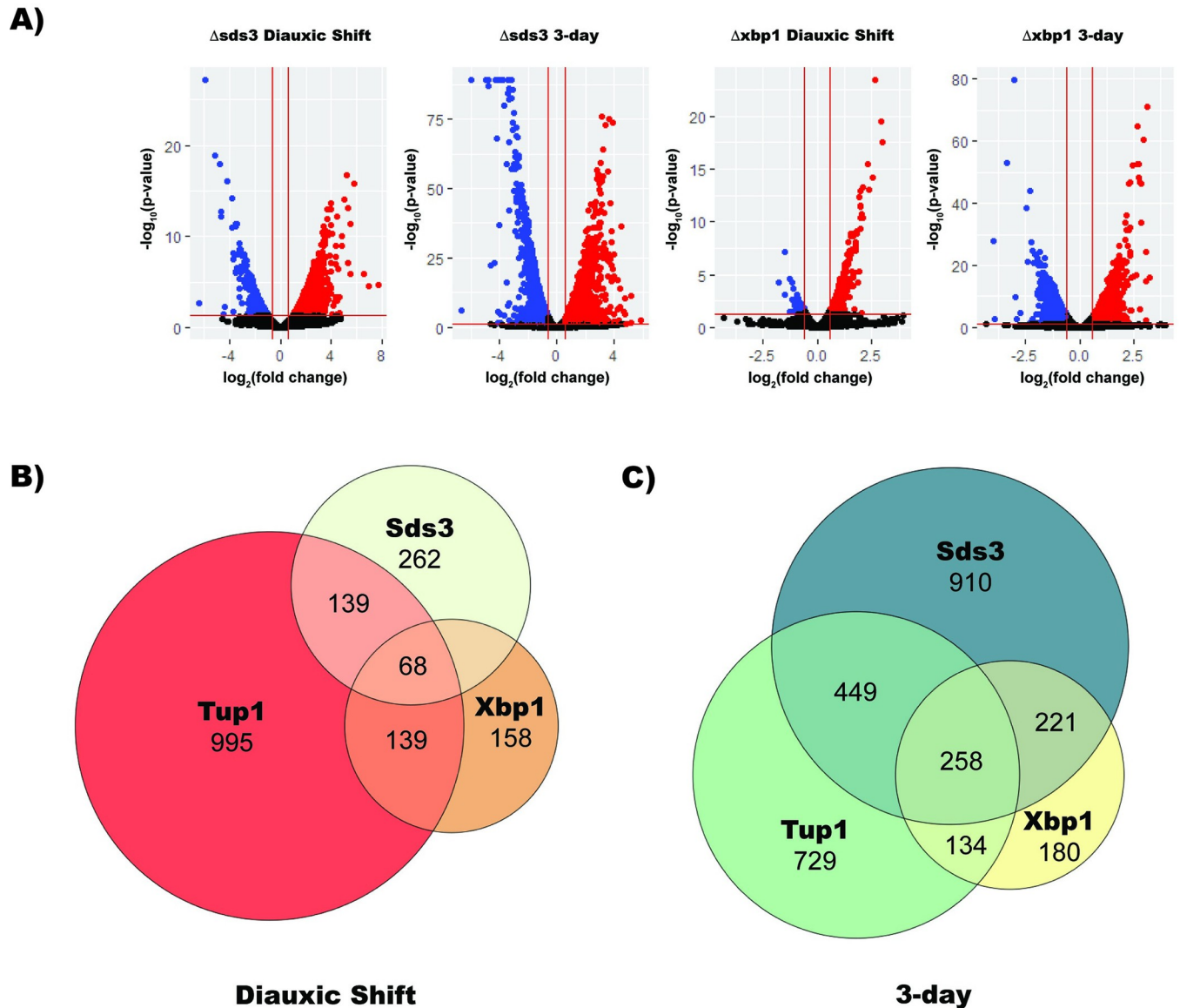
Sds3 and Xbp1 repress targets in common with Tup1

Tup1 recruits the Rpd3L complex to sites of repression through DNA-bound transcription factors [20,21,23,48]. We know that histone deacetylation during quiescence is largely Rpd3L-dependent and that Tup1 interacts with Rpd3L [40]. To explore this connection further, we first compared our Tup1 ChIP data to an existing Rpd3 ChIP dataset in quiescent cells (**S2A Fig**) [40]. We found substantial overlap in Rpd3 and Tup1 peaks, indicating that they localize to similar targets, if not interact directly. Comparing sites of Tup1 binding in 3-day cultures to Rpd3 binding sites in purified quiescent cells [40], we find that 160 of the 193 Tup1 peaks, or 94%, overlap with those of Rpd3. We also performed ChIP-Seq for the stress response factor Xbp1, which is required to recruit Rpd3 at Xbp1 motifs, and compared these data to Tup1 ChIP and found that Xbp1 and Tup1 also share binding sites (**S2B Fig**).

To elucidate the relationship between Tup1 and Rpd3 in quiescence, we knocked out Sds3, an Rpd3L-specific subunit required for deacetylation, and compared RNA-Seq datasets to that of the Tup1 knockout (**Fig 3A**). Upon deletion of Sds3 we observed that 1680 genes are differentially expressed in diauxic shift (57% repressed by Sds3 and 43% activated) and 3212 are differentially expressed during stationary phase (52% were repressed by Sds3 and 48% were activated). 734 genes that were upregulated upon Sds3 deletion in diauxic shift were also found to be upregulated during the stationary phase. A gene ontology analysis revealed that Sds3 represses many genes in common with Tup1, including those implicated in carbohydrate transport and ribosome biogenesis. Sds3 is different from Tup1 in that it represses cell cycle associated genes, which did not appear in Tup1's gene ontology analysis.

When comparing the two RNA-Seq datasets we found that during diauxic shift, 37% of genes repressed by Sds3 were also repressed by Tup1 (p < 5.5e-42) (**Fig 3B**). During stationary phase, Tup1 represses 41% of genes repressed by Sds3 (p < 1.6e-65). This suggests widespread collaboration between Tup1 and Rpd3L in repressing target genes upon glucose starvation.

The transcriptional repressor Xbp1 has been shown to recruit Rpd3L to its binding sites [40]. MACS2 [50] peak calling from our ChIP dataset on Xbp1 and Tup1 binding suggests that

A)

B)

Diauxic Shift

C)

3-day

Fig 3. Sds3 and Xbp1 Repress Targets in Common with Tup1. (A) Volcano plots of RNA-Seq differential expression data comparing Xbp1 and Sds3 deletions to wild type in both diauxic shift and stationary phase. Expression changes are based on two biological replicates. (B) Venn diagram of transcripts repressed by Tup1, Sds3, and Xbp1 in diauxic shift. (C) Venn diagram of transcripts repressed by Tup1, Sds3, and Xbp1 in stationary phase.

https://doi.org/10.1371/journal.pgen.1010559.g003

Tup1 and Xbp1 localize to similar genes (**S1 Fig**). We performed ChIP-Seq experiments in strains lacking Xbp1 and found loss of Xbp1 has no effect on Tup1 binding, demonstrating that Xbp1 does not directly recruit Tup1, even though they colocalize (**S2B Fig**). To measure the effect of Xbp1 deletion on transcriptional silencing, we deleted Xbp1 and performed RNA-Seq experiments during diauxic shift and log phase. We observed that in an Xbp1 deletion 528 genes are differentially expressed during diauxic shift, and during stationary phase 1437 genes were differentially expressed (**Fig 3A**).

Of these genes, 86% were repressed by Xbp1, and 14% were activated. During stationary phase, 51% of differentially expressed genes were repressed by Xbp1 and 49% activated. A gene ontology analysis revealed that Xbp1 is responsible for repressing genes associated with

carbohydrate metabolism during diauxic shift, while repressing carbohydrate transport and cell cycle genes during stationary phase. Xbp1 and Tup1 repress 150 (p < 3.8e-28) shared genes during diauxic shift and 379 (p < 2.8e-60) genes during stationary phase (**Fig 3C**). Xbp1 represses 153 (p < 4.8e-45) genes in common with Sds3 during diauxic shift and 455 (p <1.3e-101) during stationary phase. Xbp1 also regulates cell cycle genes along with Sds3, while Tup1 has no effect on these genes.

Tup1, Sds3, and Xbp1 are required for H3K23 deacetylation at repressed genes

Since Tup1 facilitates H3K23 deacetylation in other contexts [15], we next wanted to see if Tup1 contributes to the H3K23 deacetylation we observe during quiescence. To determine if Tup1 is required for deacetylation, we performed H3K23ac ChIP-Seq during stationary phase where Tup1, Xbp1, or Sds3 had been deleted. More than half (535) of the genes with changes in acetylation showed differential regulation by Tup1 or Sds3 in our RNA-seq data (p < 7.97e-6). Cells with the Sds3 deletion showed global hyperacetylation in the promoter region during the stationary phase (**Fig 4A and 4B**). Additionally, Δtup1 cells also showed global hyperacetylation, though not as dramatically as with the Δsds3 strain. It was difficult to see a global effect of Xbp1 deletion on acetylation levels; however, when we filtered genes with an Xbp1 motif, it appears that deletion of Xbp1 influences acetylation levels as well, although not nearly as dramatically as with loss of Sds3 or Tup1. To determine the effect of acetylation of transcription, we took the 1000 genes with the greatest changes in acetylation levels across all three mutants and compared them to genes repressed by Tup1 or Sds3 in stationary phase (**Fig 4C**). We observed a strong relationship between genes that are deacetylated in stationary phase and genes that are repressed.

Tup1 and Isw2 regulate nucleosome positions at HXT family genes

During quiescence, cells reposition their +1 nucleosomes, either to shrink the nucleosome depleted region (NDR) or to expand it. Shrinking of the NDR is generally regarded as repressive, because it presumably blocks recruitment of DNA transcription factors and RNA polymerase II. Expansion of the nucleosome NDR, on the other hand, presumably facilitates recruitment of RNA polymerase and is associated with active transcription. The vast majority of NDRs shrink during quiescence in yeast, while a few are expanded [41]. The chromatin remodeler Isw2 is known to interact with Tup1, and both proteins are required to position nucleosomes in some contexts [27,28,51]. Because Tup1 is involved in +1 nucleosome stabilization in other contexts, we performed MNase- Seq to determine if Tup1 affects the position of nucleosomes in stationary phase. We found that specifically, Tup1 and Isw2 are required to position nucleosomes at the HXT family of glucose transporter genes HXT1, HXT3, HXT8, HXT9, HXT11, HXT13, HXT15, and HXT16
(**Fig 5A**).

RNA-Seq data revealed that Isw2 is required to repress 106 genes during diauxic shift and 172 genes in stationary phase (**Fig 5B**). Isw2 represses many shared targets with Tup1: 33% of genes repressed by Isw2 are also repressed by Tup1 in diauxic shift, whereas almost half of the genes repressed by Isw2 in stationary phase are repressed by Tup1. In addition, we found a greater number of mispositioned nucleosomes in the Δisw2 strain, which had mispositioned nucleosomes in the -2, -1, +1, and +2 positions relative to the transcription start site (TSS) (**Fig 5C**). Our gene ontology analysis of the genes with mis-positioned nucleosomes in the Δisw2 deletion showed that Isw2 regulates nucleosomes in the promoters of genes involved in glucose transport, cell cycle, and DNA repair pathways in stationary phase (**Fig 5D**).

A)

H3K27 Acetylation


B)

H3K27 Acetylation

C)
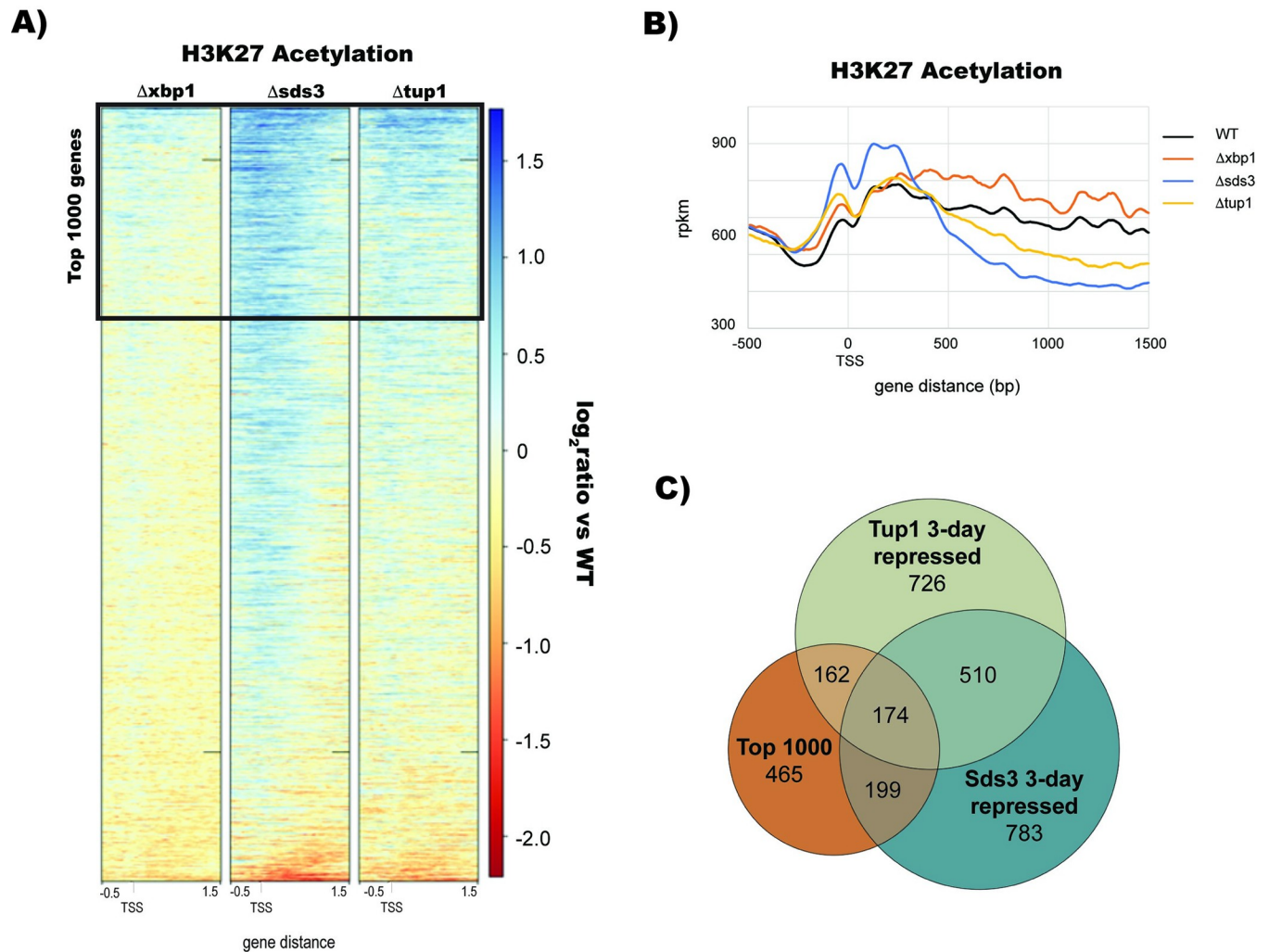
Fig 4. Tup1, Sds3, and Xbp1 are Required for H3K23 Deacetylation at Repressed Genes. (A) Heatmap showing the change in H3K23ac levels in deletion mutants compared to wild-type across all yeast genes. (B) H3K23ac profile levels across gene promoters, integrated across all yeast genes. (C) Venn diagram comparing the 1000 genes with the largest change in H3K23ac to genes repressed by Tup1 and Sds3 in stationary phase.

https://doi.org/10.1371/journal.pgen.1010559.g004

Deletion of Tup1 or Sds3 leads to morphological defects in stationary phase

Due to the multimeric nature of the Tup1-Ssn6 complex, it has been hypothesized that Tup1 may act as a scaffold for long-distance chromatin interactions. We know that during quiescence there are large scale chromatin folding events in yeast [52]. We have biochemical evidence that Tup1 may regulate chromatin folding in vitro; however, it is unknown whether this occurs in vivo. We initially wondered if deleting Tup1 would lead to less compaction of chromatin and sought to determine if Δtup1 cells had larger nuclei using fluorescence microscopy and DAPI staining. Although we failed to detect statistically significant changes in nuclei size, we found that Δtup1 cells showed multiple DAPI puncta not observed in wild type cells (**Fig 6A and 6B**).

Deletion of Sds3 did not cause this phenotype; however, Δsds3 cells were often misshapen, which we termed "peanut shaped cells" (**Fig 6C**). Peanut shaped cells have been observed in other mutants, particularly mutants involved in schmoo formation such as AFR1, PEA2, and
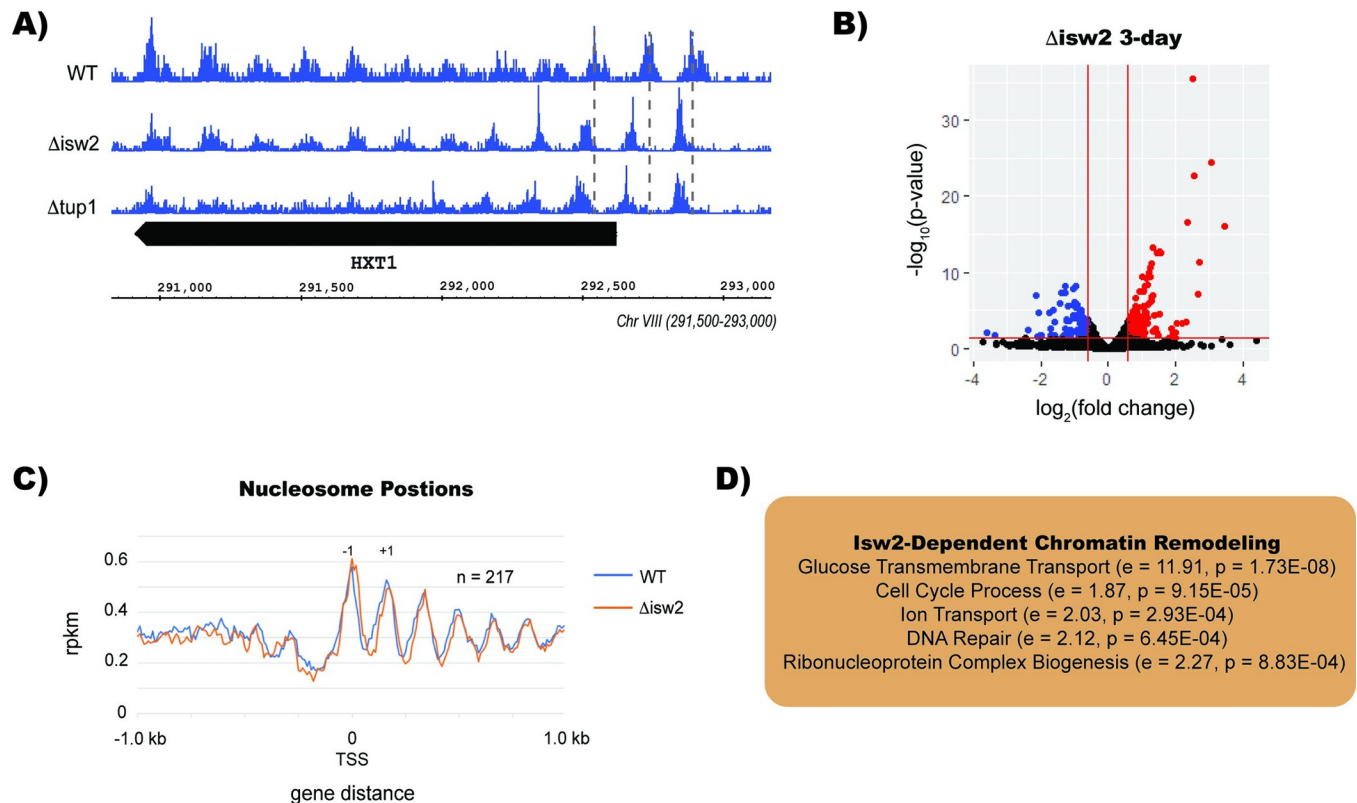
Fig 5. Tup1 and Isw2 Regulate Nucleosome Positions at HXT Family Genes. (A) Integrated Genome Browser (IGB) tracks of MNase-Seq in wild type, Δisw2, and Δtup1 in stationary phase. Dashed gray lines indicate wild type nucleosome positions. (B) Volcano plot of Δisw2 deletion in stationary phase demonstrating shifted nucleosomes at the HXT1 locus. (C) MNase-Seq dyad signal across 217 genes with shifted nucleosomes in Δisw2 during stationary phase. "-1" indicates the first nucleosome upstream of the TSS, while "+1" indicates the first nucleosome downstream of the TSS. (D) Gene ontology terms for genes with shifted nucleosome positions in Δisw2 yeast at stationary phase, with relative enrichment (e) and p- value (p) indicated for each term.

https://doi.org/10.1371/journal.pgen.1010559.g005

SPA2 [53]. While Sds3 does not appear to significantly regulate the expression of these genes, Sds3 is involved in regulating the cell cycle, bud site selection, and cell wall organization. While the phenotype between Δsds3 cells and Afr1 mutant appear similar, it is likely caused by different types of misregulation. We did not observe any changes in Δisw2 yeast compared to wild type yeast. The morphological defects observed in both Δtup1 and Δsds3 yeast suggest a potential mitotic defect, leading to aberrant distribution of DNA within nuclei in Δtup1 cells and abnormal cell division in the Δsds3 mutant. While we were unable to further investigate this phenomenon, these findings may be of interest to other researchers.

Discussion

Tup1 plays a key role in regulating large scale transcriptional responses to environmental conditions in yeast [20]. Our ChIP-Seq studies with epitope-tagged Tup1 revealed that when glucose is depleted during the diauxic shift, Tup1 releases from numerous chromatin sites where it is bound in log phase and binds at new positions that persist into the stationary phase. Tup1 binds some other sites in both log phase and during diauxic shift, typically associated with genes involved in cell wall organization. During log phase, Tup1 is bound to the promoters of ribosomal subunit proteins and tRNAs, which are actively transcribed at this stage but become repressed during diauxic shift; it seems that Tup1 is involved in both gene activation and repression. During diauxic shift, Tup1 relocalizes to genes associated with carbohydrate

A)

B)

C)
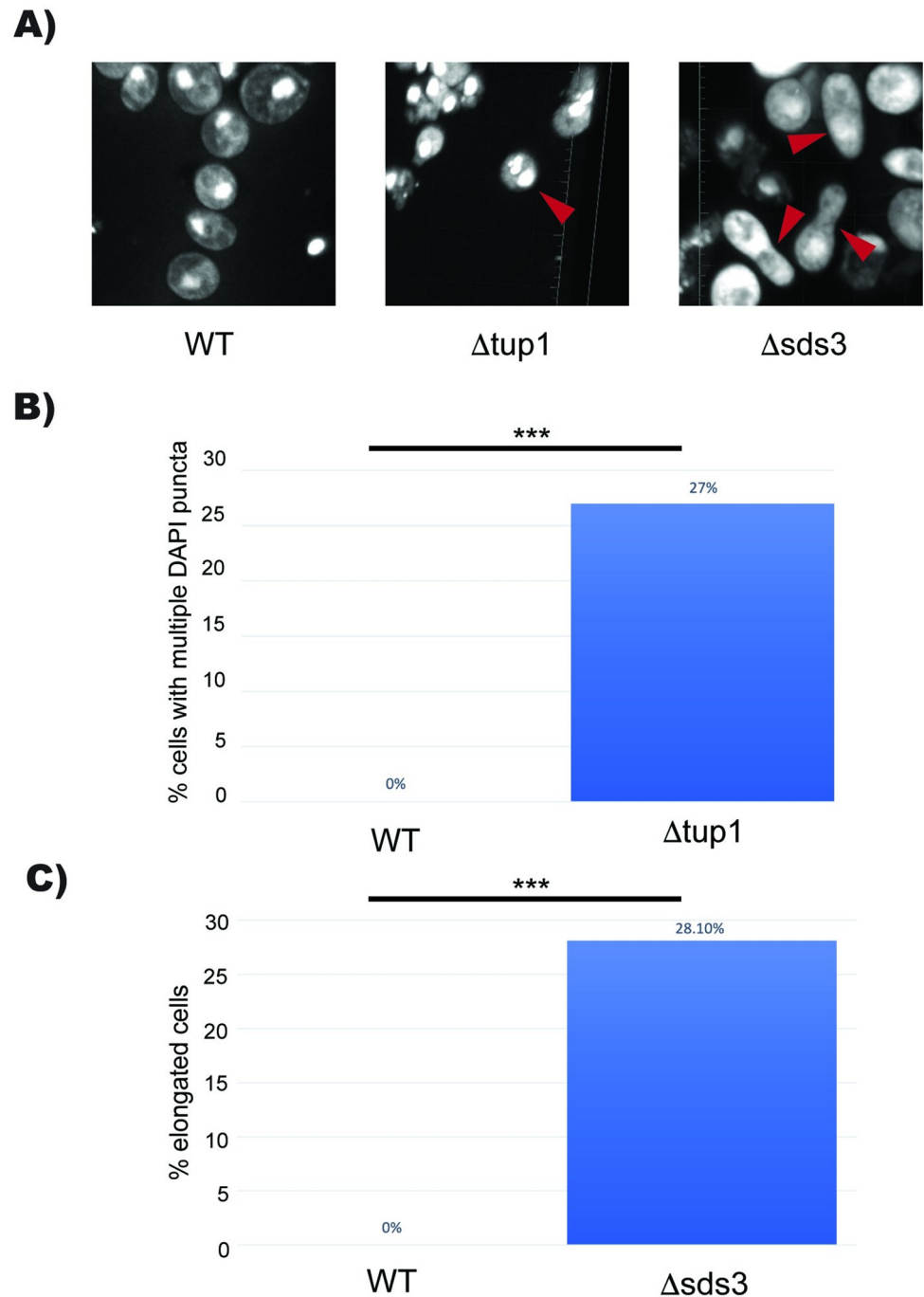
Fig 6. Deletion of Tup1 or Sds3 Leads to Morphology Defects in Stationary Phase. (A) Fluorescence microscopy of DAPI stained nuclei across the genome at 67x magnification in wild type, Δtup1, and Δsds3 yeast. (B) Quantification of Δtup1 cells with multiple DAPI puncta. WT n = 100, Δtup1 n = 48. (C) Quantification of peanut-shaped cells in Δsds3 yeast. WT n = 100, Δsds3 n = 64. *** $p < 0.05$.

https://doi.org/10.1371/journal.pgen.1010559.g006

metabolism and transport, as well as factors that convert ADP to ATP, zinc transporters, and DNA-binding transcription factors; Tup1 relocalization to these genes represses their expression. The sites occupied by Tup1 regardless of glucose availability all become derepressed in a Tup1 knockout strain, indicating that Tup1 represses these targets. We suspect that repression

of transcription factors by Tup1 may play a role in its ability to affect transcription of more factors in addition to those directly associated with its binding sites. Additionally, because Tup1 does not directly interact with DNA, we suspect that ChIP fails to reveal every instance of Tup1 binding.

Tup1 null mutants fail to repress many of the genes required for diauxic shift and establishment of quiescence. Many of the targets that are repressed/activated by Tup1 account for characteristics of quiescent cells. For example, common hallmarks of quiescent cells are fewer ribosomes, stalled translation, cell wall reorganization, and repression of metabolism. Our RNA-Seq data indicate that Tup1 is required to repress genes associated with all of these processes, demonstrating its role in regulating the transition to quiescence. Li et. al performed a genetic screen for factors that are required for quiescence in yeast. We found that Tup1 regulates more than 56% of these factors, further demonstrating the importance of Tup1 in regulating quiescence.

Tup1 regulates metabolism by simultaneously repressing genes involved in RNA, lipid, amino acid, and carbohydrate biosynthetic processes and activating the glyoxylate cycle and fatty acid metabolism. Transmembrane transporters of amino acids, carbohydrates, fatty acids, and metals (specifically magnesium, zinc, copper, and iron) are repressed by Tup1. We also find that two of the three yeast aquaporins are repressed by Tup1. It has been observed in other organisms that transmembrane transport is related to cellular proliferation [54,55]. These findings indicate that yeast cells repress the vast majority of transmembrane transporters, which likely allows the cells to maintain a controlled intracellular environment in a context where metabolism is dramatically slowed.

The importance of the Rpd3 complex in establishing a quiescent state has been well demonstrated, and one factor that recruits Rpd3 is the transcription factor Xbp1 [40]. Xbp1 and Rpd3 share many common targets of repression with Tup1, while simultaneously having targets independent of Tup1. For example, Tup1 and Sds3 both strongly repress tRNA processing factors, ribosomal subunits, transmembrane transport, sugar catabolism, and cell wall components. Xbp1 and Tup1 overlap in their repression of transmembrane transport genes and sugar metabolism. However, Xbp1 and Sds3 strongly repress cell cycle genes, which are unaffected by Tup1.

Histone deacetylation is strongly associated with transcriptional repression in quiescence [40] and we demonstrated the importance of Tup1, Xbp1, and Sds3 to facilitate histone deacetylation. Whether or not histone deacetylation is the main driving force of transcriptional repression is up for debate. We are only able to detect changes in histone deacetylation three days into stationary phase, which raises the possibility that histone deacetylation is not the main driving force in repressing transcription. However, recent findings demonstrate that the acetylome can change within 5 minutes of glucose depletion, so perhaps changes in the acetylome during diauxic shift are too subtle for us to detect [56,57]. We know that Tup1 and Rpd3 have repressive activities outside of histone deacetylation [15] but it is difficult to decipher which mechanism is employed to repress targets. Overall, there is a strong correlation between genes that are repressed and those that lose their acetyl histone marks.

Tup1 and Isw2 both coordinately regulate nucleosome positions in the promoter regions of HXT family genes. Our RNA-Seq dataset revealed that these genes are also repressed by Tup1 and Isw2, suggesting that repositioning of nucleosomes by Isw2 and Tup1 at these genes leads to repression. Interestingly, these are the only genes in which both Tup1 and Isw2 affect nucleosome positions; deletion of Tup1 has little effect on the positions of nucleosomes at any other genes. We see a greater number of nucleosomes that are affected by Isw2 in genes involved in DNA repair pathways, glucose transport, and cell cycle process. We found that in a Sds3 knockout, cells form peanut shapes, indicative of a cell attempting to divide but ultimately

failing to complete the process. Sds3 regulates many cell cycle genes, and it seems likely that failure to repress key cell cycle genes leads to the incomplete cell divisions we observed.

The multiple DAPI puncta observed in Tup1 knockout cells warrant further investigation. One possibility is that these cells have multiple nuclei or fragments of nuclei, which could be the result of a failure to properly segregate chromosomes during mitosis. Another possibility is these puncta are fragments of a broken-down nucleus, which is the result of cell cycle dysregulation. In any case, the observation highlights the importance of Tup1 in regulating the exit from the cell cycle. Taken together these results indicate that Tup1 is critical for gene repression in the exit from the cell cycle and establishment of quiescence.

It has been demonstrated that the Tup1 homologue GRG5 is critical for embryonic stem cell fate decisions in mice [58]. Additionally, TLE1 is associated with many cancers in humans, including synovial carcinoma, lung cancer, breast cancer, glioblastoma, gastric cancer, and pancreatic cancer [38]. This indicates a role of Tup1/Groucho/TLE family proteins in determining cell fate in higher eukaryotes. Perhaps a conserved role of Tup1 family proteins is to regulate entry and exit from the cell cycle, which may explain why dysregulation of Groucho of TLE in higher eukaryotes leads to cancer.

Materials and methods

Generation of deletion strains

All yeast strains were generated from the parent strain *S. cerevisiae* W303 RAD5+ (ATCC 208352). Null mutants were generated by replacing the gene of interest with antibiotic resistance markers amplified from pAG vectors [59]. FLAG- and Myc- tagged strains were made from a pFA6a vector containing their respective sequences. We then inserted the tags through homologous recombination of PCR products using selectable drug markers [59].

Growth conditions

S. cerevisiae W303 cultures were streaked from glycerol stocks onto yeast extract peptone dextrose (YPD) plates and grown at 30˚ C. Individual colonies were picked and used to inoculate 25 mL YPD with shaking at 30˚ C. These cultures were grown to an O.D. of 0.6 to 0.8 for log phase cultures. Diauxic shift cultures were obtained by monitoring glucose levels with glucose test strips (Precision Laboratories). Cells were harvested two hours after there was no detectable glucose. Stationary phase cultures were prepared by growing yeast for three days in YPD medium.

Chromatin immunoprecipitation

Chromatin immunoprecipitation was performed as previously described [60]. 100 OD-mL of cells were crosslinked in 1% formaldehyde for 20 minutes at 30˚ C. Cells were then quenched with a final concentration of 125 mM glycine, pelleted, and frozen at -80˚ C. Cells were lysed in a Bead Beater (Biospec) for two minutes with acid- washed glass beads, diameter 425–600 m (Sigma Aldrich) in the presence of protease inhibitors (Proteoloc Protease Inhibitor Cocktail, Expedeon) and then sheared in a Bioruptor sonicator for a total of 30 min (high output 30 sec on 30 sec off for 10 minutes 3x) and then centrifuged. The sheared chromatin supernatant was incubated with antibodies bound to G protein beads (Invitrogen). The crosslinks were reversed, overnight at 65˚ C and the sample was treated with 20 g RNase A for two hours at 45˚ C and 100 g Proteinase K for *4* hours at 55˚ C, and then purified using Qiagen MinElute columns. DNA samples were quantified using a Qubit fluorescence assay and libraries were prepared using a NuGEN Ovation Ultralow kit. Sequencing was performed by the University

of Oregon Genomics and Cell Characterization Core Facility on an Illumina NextSeq500 on the 37 cycle, paired-end setting, yielding approximately 10–20 million paired- end reads per sample.

RNA extraction

Cells were removed from -80˚ C and ground with a mortar and pestle in liquid nitrogen. RNA was extracted using hot acid-phenol [61] and cleaned up using the RNeasy kit (Qiagen). Libraries were prepared using the NuGEN Universal Plus mRNA kit. Sequencing was performed by University of Oregon Genomics and Cell Characterization Core Facility on an Illumina NextSeq500 with 37 cycles of paired-end setting. Paired end reads were filtered and aligned to the *S. cerevisiae* sacSer3 genome using bowtie2 [62]. Differential expression analysis was performed using DESeq2 [63].

Micrococcal nuclease digestion

We utilized our rapid MNase protocol [64]. In short, cross-linked cells were permeabilized by zymolyase digestion then treated with MNase and Exonuclease III. Next, the samples were treated with RNaseA and Proteinase K and purified using the Qiagen MinElute PCR Cleanup kit.

DAPI staining and fluorescence microscopy

Staining and microscopy was performed as described by [52]. Cells were fixed in 3.7% formaldehyde for 20 min at 4˚ C in 0.1 M KPO4 pH 6.4 buffer. Cells were washed twice in sorbitol citrate (1.2 M sorbitol, 100 mM K2HPO4, 36.4 mM citric acid) and incubated with 2.5 μg of Zymolyase for 30 minutes. Cells were added to polytetrafluoroethylene (PFTE) slides with 0.1% polylysine then washed with ice cold methanol and acetone. Next 5 μL of DAPI mount (0.1 μg/ml DAPI, 9.25 mM p-phenylenediamine, dissolved in PBS, and 90% glycerol) was added to the well. Images were taken on a Zeiss LSM 880 confocal microscope with Airyscan. Images were analyzed and processed using Imaris software (Oxford Instruments). Two biological replicates were used for each strain.

Computational analysis

All alignments were performed using Bowtie2 [62]. Further analysis was performed using deepTools including generation of heatmaps [65]. For ChIP, data was normalized to RPKM and gene tracks were visualized using Integrated Genome Browser [66]. Peak picking from ChIP data was performed using MACS2 [50]. Venn diagrams were generated using euler.com [67]. Motif analysis was performed using SEA in MEME-suite [47]. Gene ontology was performed using Gorilla [68]. We chose the two unranked lists option with our target set being genes that were present in our peak calling or genes that were differentially expressed in our RNA-seq datasets. Our background set included all transcripts that were detected in RNA-seq. Additionally we chose all enriched GO terms.

Supporting information

S1 Fig. Deletion of Tup1 causes clumping of yeast cells. WT (left) and Δtup1 (right) yeast grown to log phase in YPD.
(TIF)

S2 Fig. Rpd3, Xbp1, and Tup1 Colocalize in Glucose-Starved Yeast. (A) Integrated Genome Browser (IGB) tracks representative of ChIP-Seq for Rpd3-Myc in quiescent cells (Q cells),

Xbp1-FLAG in stationary phase (3 day), and Tup1-Myc in stationary phase (3 day). Rpd3-Myc data is from McKnight, Boerma et al. 2015. (B) Venn diagram comparing peaks from Rpd3-Myc ChIP of purified Q cells and Tup1-Myc ChIP of 3-day cultures. (C) Integrated Genome Browser (IGB) tracks representative of ChIP-Seq in stationary phase (3 day) for Xbp1-FLAG, Tup1-Myc, and Tup1-Myc in a Δxbp1 background.
(TIF)

S1 Table. Motif Analysis of Tup1 ChIP in Stationary Phase (3 day). TP = The number of primary sequences matching the motif / the number of primary sequences (the percentage of primary sequences matching the motif) TP% = The percentage of primary sequences matching the motif with scores greater than or equal to the optimal match score threshold FP = The number of control sequences matching the motif / the number of primary sequences (the percentage of control sequences matching the motif) FP% = The percentage of control sequences matching the motif with scores greater than or equal to the optimal match score threshold ENR_RATIO = The relative enrichment ration of the motif in the primary vs. control sequences, defined as Ratio = ((TP+1)/(NPOS+1)) / ((FP+1)/(NNEG+1)), where NPOS is the number of primary sequences in the input, and NNEG is the number of control sequences in the input SCORE_THR = The match score threshold giving the optimal p-value. This is the score threshold used by SEA to determine the values of "TP" and "FP"
(PDF)

Acknowledgments

The authors thank the Genomics Core (GC3F) at the University of Oregon for high throughput sequencing services. The authors also thank Christine Cucinotta (Fred Hutchinson Cancer Research Center) and Hideki Tanizawa, Osamu Iwasaki, Ken-Ichi Noma for helpful discussions related to this work. Additionally we thank Christine Cucinotta and Alison Greenlaw for tracking down Rpd3 data for us.

Author Contributions

Conceptualization: Thomas B. Bailey, Eric U. Selker, Jeffrey. N. McKnight.

Data curation: Thomas B. Bailey, Laura E. McKnight.

Formal analysis: Thomas B. Bailey, Jeffrey. N. McKnight.

Funding acquisition: Jeffrey. N. McKnight.

Investigation: Thomas B. Bailey, Phaedra A. Whitty, Jeffrey. N. McKnight, Laura E. McKnight.

Methodology: Thomas B. Bailey, Jeffrey. N. McKnight, Laura E. McKnight.

Project administration: Jeffrey. N. McKnight, Laura E. McKnight.

Resources: Eric U. Selker, Jeffrey. N. McKnight.

Supervision: Eric U. Selker, Jeffrey. N. McKnight, Laura E. McKnight.

Validation: Thomas B. Bailey.

Visualization: Thomas B. Bailey, Laura E. McKnight.

Writing – original draft: Thomas B. Bailey.

Writing – review & editing: Thomas B. Bailey, Eric U. Selker, Laura E. McKnight.

References

1. Marescal O, Cheeseman IM. Cellular Mechanisms and Regulation of Quiescence. Vol. 55, Developmental Cell. 2020. https://doi.org/10.1016/j.devcel.2020.09.029 PMID: 33171109

2. Rittershaus ESC, Baek SH, Sassetti CM. The normalcy of dormancy: Common themes in microbial quiescence. Vol. 13, Cell Host and Microbe. 2013. https://doi.org/10.1016/j.chom.2013.05.012 PMID: 23768489

3. van Velthoven CTJ, Rando TA. Stem Cell Quiescence: Dynamism, Restraint, and Cellular Idling. Vol. 24, Cell Stem Cell. 2019. https://doi.org/10.1016/j.stem.2019.01.001 PMID: 30735649

4. O'Farrell PH. Quiescence: Early evolutionary origins and universality do not imply uniformity. Vol. 366, Philosophical Transactions of the Royal Society B: Biological Sciences. 2011. https://doi.org/10.1098/rstb.2011.0079

5. Valcourt JR, Lemons JMS, Haley EM, Kojima M, Demuren OO, Coller HA. Staying alive: Metabolic adaptations to quiescence. Vol. 11, Cell Cycle. 2012. https://doi.org/10.4161/cc.19879 PMID: 22510571

6. Tümpel S, Rudolph KL. Quiescence: Good and Bad of Stem Cell Aging. Vol. 29, Trends in Cell Biology. 2019. https://doi.org/10.1016/j.tcb.2019.05.002 PMID: 31248787

7. Yao G. Modelling mammalian cellular quiescence. Vol. 4, Interface Focus. 2014. https://doi.org/10.1098/rsfs.2013.0074 PMID: 24904737

8. Vallette FM, Olivier C, Lézot F, Oliver L, Cochonneau D, Lalier L, et al. Dormant, quiescent, tolerant and persister cells: Four synonyms for the same target in cancer. Vol. 162, Biochemical Pharmacology. 2019. https://doi.org/10.1016/j.bcp.2018.11.004 PMID: 30414937

9. de Virgilio C. The essence of yeast quiescence. Vol. 36, FEMS Microbiology Reviews. 2012. https://doi.org/10.1111/j.1574-6976.2011.00287.x PMID: 21658086

10. Gray JV, Petsko GA, Johnston GC, Ringe D, Singer RA, Werner-Washburne M. "Sleeping Beauty": Quiescence in Saccharomyces cerevisiae. Microbiology and Molecular Biology Reviews. 2004; 68(2). https://doi.org/10.1128/MMBR.68.2.187-206.2004 PMID: 15187181

11. Miles S, Bradley GT, Breeden LL. The budding yeast transition to quiescence. Yeast. 2021; 38(1). https://doi.org/10.1002/yea.3546 PMID: 33350501

12. Sun S, Gresham D. Cellular quiescence in budding yeast. Vol. 38, Yeast. 2021. https://doi.org/10.1002/yea.3545 PMID: 33350503

13. Yanagida M. Cellular quiescence: are controlling genes conserved? Vol. 19, Trends in Cell Biology. 2009. https://doi.org/10.1016/j.tcb.2009.09.006 PMID: 19833516

14. Allen C, Büttner S, Aragon AD, Thomas JA, Meirelles O, Jaetao JE, et al. Isolation of quiescent and nonquiescent cells from yeast stationary-phase cultures. Journal of Cell Biology. 2006; 174(1). https://doi.org/10.1083/jcb.200604072 PMID: 16818721

15. Malavé TM, Dent SYR. Transcriptional repression by Tup1-Ssn6. In: Biochemistry and Cell Biology. 2006. https://doi.org/10.1139/o06-073 PMID: 16936817

16. Conlan RS, Gounalaki N, Hatzis P, Tzamarias D. The Tup1-Cyc8 protein complex can shift from a transcriptional co-repressor to a transcriptional co-activator. Journal of Biological Chemistry. 1999; 274(1). https://doi.org/10.1074/jbc.274.1.205 PMID: 9867831

17. Proft M, Struhl K. Hog1 kinase converts the Sko1-Cyc8-Tup1 repressor complex into an activator that recruits SAGA and SWI/SNF in response to osmotic stress. Mol Cell. 2002; 9(6). https://doi.org/10.1016/s1097-2765(02)00557-9 PMID: 12086627

18. Varanasi US, Klis M, Mikesell PB, Trumbly RJ. The Cyc8 (Ssn6)-Tup1 corepressor complex is composed of one Cyc8 and four Tup1 subunits. Mol Cell Biol. 1996; 16(12). https://doi.org/10.1128/MCB.16.12.6707 PMID: 8943325

19. Sprague ER, Redd MJ, Johnson AD, Wolberger C. Structure of the C-terminal domain of Tup1, a corepressor of transcription in yeast. EMBO Journal. 2000; 19(12). https://doi.org/10.1093/emboj/19.12.3016 PMID: 10856245

20. Hanlon SE, Rizzo JM, Tatomer DC, Lieb JD, Buck MJ. The stress response factors Yap6, Cin5, Phd1, and Skn7 direct targeting of the conserved co-repressor Tup1-Ssn6 in S. cerevisiae. PLoS One. 2011; 6(4). https://doi.org/10.1371/journal.pone.0019060

21. Davie JK, Edmondson DG, Coco CB, Dent SYR. Tup1-Ssn6 Interacts with Multiple Class I Histone Deacetylases in Vivo. Journal of Biological Chemistry. 2003; 278(50). https://doi.org/10.1074/jbc.M309753200 PMID: 14525981

22. Fleming AB, Beggs S, Church M, Tsukihashi Y, Pennings S. The yeast Cyc8-Tup1 complex cooperates with Hda1p and Rpd3p histone deacetylases to robustly repress transcription of the subtelomeric FLO1 gene. Biochim Biophys Acta Gene Regul Mech. 2014; 1839(11). https://doi.org/10.1016/j.bbagrm.2014.07.022 PMID: 25106892

23. Watson AD, Edmondson DG, Bone JR, Mukai Y, Yu Y, Du W, et al. Ssn6-Tup1 interacts with class I histone deacetylases required for repression. Genes Dev. 2000; 14(21). https://doi.org/10.1101/gad.829100 PMID: 11069890

24. Wu J, Suka N, Carlson M, Grunstein M. TUP1 utilizes histone H3/H2B-specific HDA1 deacetylase to repress gene activity in yeast. Mol Cell. 2001; 7(1). https://doi.org/10.1016/s1097-2765(01)00160-5 PMID: 11172717

25. Chen K, Wilson MA, Hirsch C, Watson A, Liang S, Lu Y, et al. Stabilization of the promoter nucleosomes in nucleosome-free regions by the yeast Cyc8-Tup1 corepressor. Genome Res. 2013; 23(2). https://doi.org/10.1101/gr.141952.112 PMID: 23124522

26. Li B, Reese JC. Ssn6-Tup1 Regulates RNR3 by Positioning Nucleosomes and Affecting the Chromatin Structure at the Upstream Repression Sequence. Journal of Biological Chemistry. 2001; 276(36). https://doi.org/10.1074/jbc.M104220200 PMID: 11448965

27. Rizzo JM, Mieczkowski PA, Buck MJ. Tup1 stabilizes promoter nucleosome positioning and occupancy at transcriptionally plastic genes. Nucleic Acids Res. 2011; 39(20). https://doi.org/10.1093/nar/gkr557 PMID: 21785133

28. Zhang Z, Reese JC. Ssn6-Tup1 requires the ISW2 complex to position nucleosomes in Saccharomyces cerevisiae. EMBO Journal. 2004; 23(11). https://doi.org/10.1038/sj.emboj.7600227

29. Papamichos-Chronakis M, Conlan RS, Gounalaki N, Copf T, Tzamarias D. Hrs1/Med3 is a Cyc8-Tup1 corepressor target in the RNA polymerase II holoenzyme. Journal of Biological Chemistry. 2000; 275 (12). https://doi.org/10.1074/jbc.275.12.8397 PMID: 10722672

30. Parnell EJ, Stillman DJ. Shields up: The Tup1-Cyc8 repressor complex blocks coactivator recruitment. Genes Dev. 2011; 25(23). https://doi.org/10.1101/gad.181768.111 PMID: 22156205

31. Wong KH, Struhl K. The Cyc8-Tup1 complex inhibits transcription primarily by masking the activation domain of the recruiting protein. Genes Dev. 2011; 25(23). https://doi.org/10.1101/gad.179275.111 PMID: 22156212

32. Jennings BH, Ish-Horowicz D. The Groucho/TLE/Grg family of transcriptional co-repressors. Genome Biol. 2008; 9(1). https://doi.org/10.1186/gb-2008-9-1-205 PMID: 18254933

33. Jumper J, Evans R, Pritzel A, Green T, Figurnov M, Ronneberger O, et al. Highly accurate protein structure prediction with AlphaFold. Nature. 2021; 596(7873). https://doi.org/10.1038/s41586-021-03819-2

34. Varadi M, Anyango S, Deshpande M, Nair S, Natassia C, Yordanova G, et al. AlphaFold Protein Structure Database: Massively expanding the structural coverage of protein-sequence space with high-accuracy models. Nucleic Acids Res. 2022; 50(D1). https://doi.org/10.1093/nar/gkab1061 PMID: 34791371

35. Flores-Saaib RD, Courey AJ. Analysis of Groucho-histone interactions suggests mechanistic similarities between Groucho- and Tup1-mediated repression. Nucleic Acids Res. 2000; 28(21). https://doi.org/10.1093/nar/28.21.4189 PMID: 11058116

36. Grbavec D, Lo R, Liu Y, Greenfield A, Stifani S. Groucho/transducin-like Enhancer of split (TLE) family members interact with the yeast transcriptional co-repressor SSN6 and mammalian SSN6-related proteins: Implications for evolutionary conservation of transcription repression mechanisms. Biochemical Journal. 1999; 337(1). https://doi.org/10.1042/0264-6021:3370013 PMID: 9854018

37. Agarwal M, Kumar P, Mathew SJ. The Groucho/Transducin-like enhancer of split protein family in animal development. Vol. 67, IUBMB Life. 2015. https://doi.org/10.1002/iub.1395 PMID: 26172616

38. Yuan D, Yang X, Yuan Z, Zhao Y, Guo J. TLE1 function and therapeutic potential in cancer. Vol. 8, Oncotarget. 2017. https://doi.org/10.18632/oncotarget.13278 PMID: 27852056

39. Ogawa M, Yaginuma T, Nakatomi C, Nakajima T, Tada-Shigeyama Y, Addison WN, et al. Transducin-like enhancer of split 3 regulates proliferation of melanoma cells via histone deacetylase activity. Oncotarget. 2019; 10(3). https://doi.org/10.18632/oncotarget.26552 PMID: 30719233

40. McKnight JN, Boerma JW, Breeden LL, Tsukiyama T. Global Promoter Targeting of a Conserved Lysine Deacetylase for Transcriptional Shutoff during Quiescence Entry. Mol Cell. 2015; 59(5). https://doi.org/10.1016/j.molcel.2015.07.014 PMID: 26300265

41. McKnight JN, Breeden LL, Tsukiyama T. A molecular off switch for transcriptional quiescence. Cell Cycle. 2015; 14(23). https://doi.org/10.1080/15384101.2015.1112618 PMID: 26514179

42. Lin X, Yu AQ, Zhang CY, Pi L, Bai XW, Xiao DG. Functional analysis of the global repressor Tup1 for maltose metabolism in Saccharomyces cerevisiae: Different roles of the functional domains. Microb Cell Fact. 2017; 16(1). https://doi.org/10.1186/s12934-017-0806-6 PMID: 29121937

43. Papamichos-Chronakis M, Gligoris T, Tzamarias D. The Snf1 kinase controls glucose repression in yeast by modulating interactions between the Mig1 repressor and the Cyc8-Tup1 co-repressor. EMBO Rep. 2004; 5(4). https://doi.org/10.1038/sj.embor.7400120 PMID: 15031717

44. Reimand J, Aun A, Vilo J, Vaquerizas JM, Sedman J, Luscombe NM. M:Explorer: Multinomial regression models reveal positive and negative regulators of longevity in yeast quiescence. Genome Biol. 2012; 13(6). https://doi.org/10.1186/gb-2012-13-6-r55 PMID: 22720667

45. Williams FE, Varanasi U, Trumbly RJ. The CYC8 and TUP1 proteins involved in glucose repression in Saccharomyces cerevisiae are associated in a protein complex. Mol Cell Biol. 1991; 11(6). https://doi.org/10.1128/mcb.11.6.3307-3316.1991 PMID: 2038333

46. Williams FE, Trumbly RJ. Characterization of TUP1, a mediator of glucose repression in Saccharomyces cerevisiae. Mol Cell Biol. 1990; 10(12). https://doi.org/10.1128/mcb.10.12.6500 PMID: 2247069

47. Bailey TL, Grant CE. SEA: Simple Enrichment Analysis of motifs. bioRxiv. 2021 http://www.biorxiv.org/content/10.1101/2021.08.23.457422v1

48. Treitel MA, Carlson M. Repression by SSN6-TUP1 is directed by MIG1, a repressor/activator protein. Proc Natl Acad Sci U S A. 1995; 92(8). https://doi.org/10.1073/pnas.92.8.3132 PMID: 7724528

49. Li L, Miles S, Breeden LL. A genetic screen for Saccharomyces cerevisiae mutants that fail to enter quiescence. G3: Genes, Genomes, Genetics. 2015; 5(8). https://doi.org/10.1534/g3.115.019091 PMID: 26068574

50. Zhang Y, Liu T, Meyer CA, Eeckhoute J, Johnson DS, Bernstein BE, et al. Model-based analysis of ChIP-Seq (MACS). Genome Biol. 2008; 9(9). https://doi.org/10.1186/gb-2008-9-9-r137 PMID: 18798982

51. Zhang Z, Reese JC. Redundant mechanisms are used by Ssn6-Tup1 in repressing chromosomal gene transcription in Saccharomyces cerevisiae. Journal of Biological Chemistry. 2004; 279(38). https://doi.org/10.1074/jbc.M407159200 PMID: 15254041

52. Swygert SG, Kim S, Wu X, Fu T, Hsieh TH, Rando OJ, et al. Condensin-Dependent Chromatin Compaction Represses Transcription Globally during Quiescence. Mol Cell. 2019; 73(3). https://doi.org/10.1016/j.molcel.2018.11.020 PMID: 30595435

53. Chenevert J, Valtz N, Herskowitz I. Identification of genes required for normal pheromone-induced cell polarization in Saccharomyces cerevisiae. Genetics. 1994; 136(4). https://doi.org/10.1093/genetics/136.4.1287 PMID: 8013906

54. Peters-Regehr T, Bode JG, Kubitz R, Häussinger D. Organic osmolyte transport in quiescent and activated rat hepatic stellate cells (Ito cells). Hepatology. 1999; 29(1). https://doi.org/10.1002/hep.510290111 PMID: 9862864

55. Shyh-Chang N, Daley GQ. Metabolic switches linked to pluripotency and embryonic stem cell differentiation. Vol. 21, Cell Metabolism. 2015. https://doi.org/10.1016/j.cmet.2015.02.011 PMID: 25738450

56. Hsieh WC, Sutter BM, Ruess H, Barnes SD, Malladi VS, Tu BP. Glucose starvation induces a switch in the histone acetylome for activation of gluconeogenic and fat metabolism genes. Mol Cell. 2022; 82(1). https://doi.org/10.1016/j.molcel.2021.12.015 PMID: 34995509

57. Cai L, Sutter BM, Li B, Tu BP. Acetyl-CoA Induces Cell Growth and Proliferation by Promoting the Acetylation of Histones at Growth Genes. Mol Cell. 2011; 42(4). https://doi.org/10.1016/j.molcel.2011.05.004 PMID: 21596309

58. Chanoumidou K, Hadjimichael C, Athanasouli P, Ahlenius H, Klonizakis A, Nikolaou C, et al. Groucho related gene 5 (GRG5) is involved in embryonic and neural stem cell state decisions. Sci Rep. 2018; 8(1). https://doi.org/10.1038/s41598-018-31696-9 PMID: 30214018

59. Longtine MS, McKenzie A, Demarini DJ, Shah NG, Wach A, Brachat A, et al. Additional modules for versatile and economical PCR-based gene deletion and modification in Saccharomyces cerevisiae. Yeast. 1998; 14(10). https://doi.org/10.1002/(SICI)1097-0061(199807)14:10<953::AID-YEA293>3.0.CO;2-U PMID: 9717241

60. Rodriguez J, McKnight JN, Tsukiyama T. Genome-wide analysis of nucleosome positions, occupancy, and accessibility in yeast: Nucleosome mapping, high-resolution histone chIP, and NCAM. Curr Protoc Mol Biol. 2014; 2014. https://doi.org/10.1002/0471142727.mb2128s108 PMID: 25271716

61. Uppuluri P, Perumal P, LaJean Chaffin W. Analysis of RNA species of various sizes from stationary-phase planktonic yeast cells of Candida albicans. FEMS Yeast Res. 2007; 7(1). https://doi.org/10.1111/j.1567-1364.2006.00143.x PMID: 17311589

62. Langmead B, Salzberg SL. Fast gapped-read alignment with Bowtie 2. Nat Methods. 2012; 9(4). https://doi.org/10.1038/nmeth.1923 PMID: 22388286

63. Love MI, Huber W, Anders S. Moderated estimation of fold change and dispersion for RNA-seq data with DESeq2. Genome Biol. 2014; 15(12). https://doi.org/10.1186/s13059-014-0550-8 PMID: 25516281

64. McKnight LE, Crandall JG, Bailey TB, Banks OGB, Orlandi KN, Truong VN, et al. Rapid and inexpensive preparation of genome-wide nucleosome footprints from model and non-model organisms. STAR Protoc. 2021; 2(2). https://doi.org/10.1016/j.xpro.2021.100486 PMID: 34041500

65. Ramírez F, Ryan DP, Grüning B, Bhardwaj V, Kilpert F, Richter AS, et al. deepTools2: a next generation web server for deep-sequencing data analysis. Nucleic Acids Res. 2016; 44(W1). https://doi.org/10.1093/nar/gkw257 PMID: 27079975

66. Freese NH, Norris DC, Loraine AE. Integrated genome browser: Visual analytics platform for genomics. Bioinformatics. 2016; 32(14). https://doi.org/10.1093/bioinformatics/btw069 PMID: 27153568

67. Larsson J, Gustafsson P. {eulerr}: Area-Proportional Euler and Venn Diagrams with Ellipses. Vol. 2116, Proceedings of {{International Workshop}} on {{Set Visualization}} and {{Reasoning}}. 2018. https://cran.r-project.org/package=eulerr

68. Eden E, Navon R, Steinfeld I, Lipson D, Yakhini Z. GOrilla: A tool for discovery and visualization of enriched GO terms in ranked gene lists. BMC Bioinformatics. 2009; 10. https://doi.org/10.1186/1471-2105-10-48 PMID: 19192299